

## Crystallochemical properties of natural and modified clays from Maroua-Cameroon used in water treatment processes

ZeBilo'oPhylemon<sup>b</sup>, NdjeumiChrisdelChancelice<sup>a\*</sup>,  
MoutheAnombogoGhislainArnaud<sup>a</sup>, MaicaneanuAndradaSanda<sup>d</sup>, Sieliechi  
Joseph Marie<sup>c</sup>, KamgaRichard<sup>d</sup>

<sup>a</sup> - National Advanced School of Engineering of Maroua - University of Maroua PO Box 46 Maroua-Cameroon

<sup>b</sup> - Faculty of mines and petroleum industry - University of Maroua PO Box 46 Maroua-Cameroon

<sup>c</sup> - National advanced School of agro-industrial Sciences - University of Ngaoundere PO Box 455 Ngaoundere - Cameroon

<sup>d</sup> - Madia Department of Chemistry, Indiana University of Pennsylvania, Indiana PA 15705, USA

\* Corresponding author.

### ABSTRACT

The use of a clay in a defined area is dependent on its chemical composition and its structural, textural, and superficial properties. The search for these characteristics was the main purpose of this study. Acid activation (A05) and pillaring processes (APA) were implemented to show their effect on the structure and clay properties by using X-ray diffractometry, IR spectroscopy, thermal analysis, elemental chemical analysis, and gas-adsorption-desorption measurements. The analyzes carried out showed that the clay is of the swelling type and its main constituent is montmorillonite. Acid activation and pillaring treatment lead to changes in their structural, textural, and surface energy properties, while the exchangeable cations ( $\text{Ca}^{2+}$ ,  $\text{Na}^+$ ) are removed. It was also observed that Mg, Fe, and K atoms are part of clay lattice. Indeed, the acid treatment partially destroys the basic structure of the clay and pillaring creates an Al bridge between the layers of montmorillonite. The specific surfaces of raw clay (ANB), A05, and APA are 112, 77, and 99  $\text{m}^2 \cdot \text{g}^{-1}$  respectively, for a pore diameter centered around 50 Å for ANB and increasing with the different treatments, i.e. 78 Å for A05 and 81 Å for APA. The pore size distribution shows that the acid treatments and pillaring process promote the formation of mesopores by more than 60% in APA in the detriment of the majority micropores (58%) in ANB. This indicates that pillared clay is presented by its characteristics as the best matrix to use as an adsorbent in water treatment.

**Key words:** Clay, Pillaring process, Acid activation, Crystallochemical properties, Montmorillonite, Water treatment

Date of Submission: 11-01-2023

Date of acceptance: 27-01-2023

### I. INTRODUCTION

The end of the 20th century was marked by a significant reduction in water resources. This reduction was attributed to natural phenomena such as drought or water pollution. Water pollution is related to anthropogenic activities such as using surface water as spillways for pollutants (Eggenet al., 2014; Gerecke et al., 2002; Lefebvre and Moletta, 2006; Michael et al., 2013). Therefore, inexpensive and sustainable methods for the treatment of wastewater is an imperative to protect environment. Very often, adsorption is used as a method for the removal of organics matters and metals in water as well as pre or final treatment (Yadanaparthiet al., 2009, Kwon et al., 2010;

Basuet al., 2006; Srivastava et al., 2006). It requires the use of adsorbent materials including activated carbon (Ahmaruzzaman, 2010; Alsbaiet al., 2016; Dias et al., 2007 ; Stackelberget al., 2007 ; Delgado et al., 2012; Rossneret al., 2009; Snyder et al., 2007), zeolite (Nan et al., 2018, Damjanovicet al., 2010; Rakicet al., 2010), alumina (Wibulswaset al., 1998, Ndjeumiet al., 2015); biosorbents (Li et al., 2020 ; Menyaet al., 2018; Ibisi and Asoluka, 2018 ; Moutheet al., 2016, Boldizsaret al., 2014), or clays (Anuradhaet al., 2019; Adjia, 2012, Chatain, 2004). The most used adsorbents in industrial processes for the treatment of drinking water are activated carbon and clays (Dimple, 2014). However, activated carbons are much more expensive to produce and

regenerate than clays. Adsorption on clays appears therefore as one of the most promising method of water treatment process because of its efficiency, its easy implementation, and its low costs (Babel and Kurniawan, 2003; Mohan *et al.*, 2014). Various clay minerals are found in abundance in Cameroon with a variability of the geological base depending on location (Njoya *et al.*, 2001, 2006).

The use of clay depends on chemical composition, structural, textural, and superficial properties. These characteristics depend on the origin of the clay and the preliminary treatments (Bouras, 2003, Villieras *et al.*, 2002). The determination of the mineralogy and crystallochemical phases as well as the superficial properties of clay materials constitute a prerequisite to understand phenomena that take place during their modifications and their application in wastewater treatment.

The aim of this study is to classify the typological aspect of clay from characteristics likely to influence the adsorption phenomena and to observe the influence of various modifications (acid activation and pillaring) on the basic structure of the clay.

## II. MATERIAL AND METHODS

### Clays sampling, fractionation, and modification

Aggregate removal was done in the dried Mayo Kaliao bed located in the dry tropical zone of Cameroon, crossing the town of Maroua. The geographical coordinates of the sampling point obtained by GPS are 10.59357N, 14.28688E and 405 m altitude. Soil samples were kept in high density polyethylene bags and transported to the laboratory. Samples were crushed, manually ground, and dried at room temperature for 72 hours. They were then sieved to separate coarse particles and unwanted constituents. Thus, dry and wet sieving were consecutively performed to obtain size less than 50  $\mu\text{m}$ . The obtained fractions were dried in an oven at 105 °C for 24 hour. After drying, the soil samples were treated with hydrogen peroxide, 30 %, according to the method of Petard (1993) to remove the organic matter. After this treatment, the product obtained was further fractionated by gravitational sedimentation according to Stokes' law and two fractions of particle size <2  $\mu\text{m}$  and another of size between 2 and 50  $\mu\text{m}$  were obtained. These fractions were subjected to acid activation and pillaring treatments.

The method used for acid activation of clays is that of Soumaya *et al.* (2009). 100 g portions of clay were contacted with 500 mL of sulfuric acid solution of various concentrations (0.5 M, 1 M, and 2 M) in 1000 mL beakers. The mixture was stirred and allowed to stand at room temperature for 24

hours. At the end of this period, the mixture was filtered on n°4 Wattman filter paper, then the pellet was washed with bi-distilled water until a pH 7. The washing was considered complete when the filtrate sulphates no longer react with the barium chloride solution. Acid activated clay obtained was dried in an oven at 105 °C, then ground with a porcelain mortar, and conditioned.

For pillaring, the method of preparation used was a combination of those applied by Bouras (2003), Unuabonahet *et al.* (2008), Reddy *et al.* (2009) and Nguemtchouin (2012). The aluminum hydroxide solution, used as a pillaring solution, is prepared by adding a solution of 10<sup>-1</sup> M NaOH to a solution of AlCl<sub>3</sub>·6H<sub>2</sub>O 10<sup>-1</sup> M. This addition is done with a low flow rate (1 mL·min<sup>-1</sup>) to reduce the risk of precipitation of aluminum hydroxide. The volume of the two reagents used is determined to obtain an OH<sup>-</sup>/Al<sup>3+</sup> hydrolysis ratio of 2.4. This addition is carried out without modification of pH and the solution obtained is stored and aged for 48 hours before application. Finally, the pillaring is carried out by mixing the suspension of homo-sodic clay at 0.5 wt.% with the pillaring solution. The addition of both solutions was done with a peristaltic pump under continuous stirring at 8 mL·min<sup>-1</sup>. The volume of reagents was calculated for a molar ratio Me/clay-Na of 80 mmol·g<sup>-1</sup>.

The mixture of ionic solution and clay was kept under stirring for 24 hours to allow the insertion of the polycations in between the clay sheets. Later, the mixture was separated through centrifugation at 7000 rpm for 30 min, washed several times with double-distilled water, filtered under vacuum, and dried at 70°C in an oven. The product was finally ground and kept in glass vials until further use.

### Clay characterization

The X-ray diffraction (X-RD) data were obtained using a D8 Bruker diffractometer with CoK $\alpha_1$  radiation ( $\lambda = 1.789 \text{ \AA}$ ). Spectra were recorded on oriented and unoriented samples. The detection limit for a given crystalline phase is estimated at around 1% in mass. Ethylene glycol and heat treatments (550°C) were used to provide additional information essential for the identification of clay minerals.

Infrared spectra were recorded using an IFS 55 Bruker Fourier transform IR spectrometer equipped with an MCT detector (6000-600cm<sup>-1</sup>) cooled a 77K and in diffuse reflectance (Harrick attachment) mode. The amount of clay used was 70 mg dispersed in 370 mg KBr.

TEM observations were carried out with a Philips CM20 microscope equipped with an EDS detector. SEM analysis was carried out on a Hitachi 2500 LB SE microscope equipped with a Kevex Delta EDS

spectrometer. SEM were used to assist in the identification of individual accessory minerals incorporated in the clay samples by comparing their morphological characteristics with their elemental compositions.

Chemical analyses were performed on raw and treated clays forms. The major elements were determined by inductively coupled plasma atomic emission spectroscopy (ICP-AES) while trace elements and rare earths elements were determined by inductively coupled plasma mass spectrometry (ICP-MS).

Specific surfaces areas (SSA) were determined from adsorption data by applying the Brunauer-Emmet-Teller (BET) equation and using  $16.3\text{\AA}^2$  for the cross-sectional area of nitrogen. In the present study, the error in the determination of the SSA was estimated as  $\pm 1\text{m}^2/\text{g}$ . Micropores volumes and non-microporous surface areas were obtained using the t-plot method proposed by De Boer and al., (1996). Pore size distributions were calculated on the

desorption branch using the Barrett-Joyner-Halenda method, assuming slit-shaped pores.

The differential thermal analysis diagrams were obtained on 47 mg of sample with thermo-balance  $\pm 0.1$  mg. The differential thermal analysis (DTA) and thermogravimetric analysis (TGA) were obtained simultaneously with a Mettler Toledo 851 thermal analyser at a heating rate of  $10^\circ\text{C}/\text{min}$ , using air atmosphere and in the  $20\text{-}1200^\circ\text{C}$  temperature range.

### III. RESULTS AND DISCUSSION STRUCTURAL PROPERTIES OF CLAYS

#### Chemical analysis

Chemical analysis of raw, acid activated, and pillared clays has shown that oxygen is the most abundant element as all the other elements are in their oxide form. Different samples are mainly constituted of silica, aluminium, potassium, and iron oxides (Table 1).

**Table 1:** Chemical composition of clays

Element	Raw clay (ANB)	Activated clay (A05)	Pillared clay (APA)
Si	30.05	33.09	28.50
Al	16.23	17.25	18.12
O	45.24	40.17	46.78
Fe	4.88	6.56	4.39
Mg	1.32	1.15	1.11
K	0.79	1.07	0.71
Ca	0.80	/	/
Na	0.22	/	0.42
Ti	0.58	0.84	0.44
V	0.03	0.02	/
Co	0.16	/	/
C	1.84	/	/

Raw clays sample clay contain carbon, due to the presence of organic matter which would be completely destroyed during acid and pillaring treatments. Acid treatment and pillaring of clay lead to the complete removal of  $\text{Ca}^{2+}$  and  $\text{Na}^+$ , whereas only 13% of magnesium is eliminated during this treatment. This implies that  $\text{Ca}^{2+}$  and  $\text{Na}^+$  are the main exchangeable cations whereas  $\text{Mg}^{2+}$  is part of the structure of the clay. This is similar to the findings of Adjiaet al. (2013), which demonstrated that magnesium is part of the structure of alluvial clays in the Far North region of Cameroon.

The pillaring treatment favored the decrease of the Si/Al ratio due to the formation of aluminum bridges between the clay sheets (Bouras, 2003; Talidi, 2006).

The Si/Al ratio is of the order of 1.85 for each of the soil fractions. It indicates that the soil

fractions studied are made up of swelling clays (Bouras, 2003; Nguemchouin, 2012).

#### X-ray diffraction

The X-ray diffractograms of the two fractions ( $2\ \mu\text{m}$  and  $50\ \mu\text{m}$ ) of raw clay are presented in Figure 1. These diffractograms have the same appearance as one of clay minerals. The  $2\ \mu\text{m}$  particle peaks intensity is greater than that of the  $50\ \mu\text{m}$ . The lower intensity of the  $50\ \mu\text{m}$  diffractogram peaks can be attributed to the smaller concentration of minerals in this fraction. In fact, this sample contains, in addition to clay, a high proportion of feldspars, which are amorphous materials. In addition, the  $50\ \mu\text{m}$  particle peaks shows an angle corresponding to orthoclase at  $2\theta = 32.8^\circ$  and to illite at  $2\theta = 33.6^\circ$ .

The presence of the peaks at diffraction angles of  $2\theta = 11.6^\circ, 16.9^\circ, 23.5^\circ, 41.6^\circ$  corresponds to the inter-lamellar distances of 9.9, 6.1, 4.4, and 2.5 Å respectively characteristics of a montmorillonite. The 2 µm clay fraction also contains by the illite identified by its peak at  $2\theta =$

$10^\circ$  which corresponds to an equidistance  $d = 10.27\text{Å}$ . This diffractogram also shows peaks  $2\theta = 13.9^\circ, 28.7^\circ$  and  $49.2^\circ$  ( $d = 7.4\text{Å}, 3.6\text{Å}$  and  $2.1\text{Å}$ ) corresponding to kaolinite. The crude clay here is therefore predominantly composed of montmorillonite.

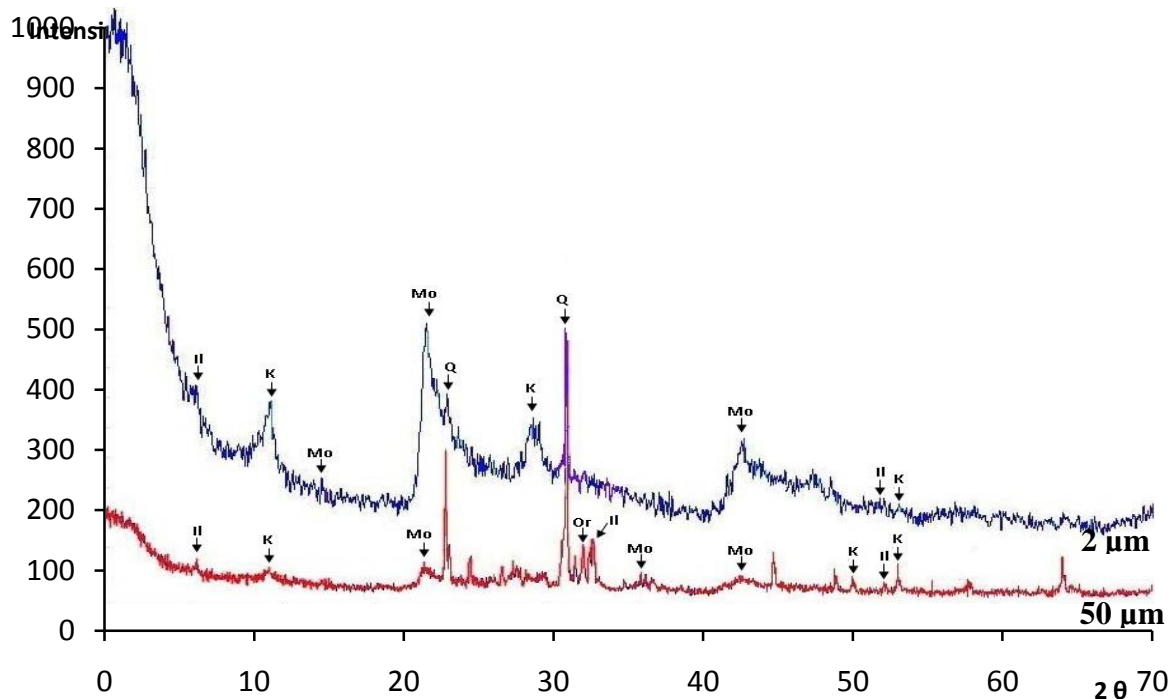


**Figure 1:** Diffractograms of 2 µm and 50µ m clay fractions. Mo = montmorillonite, Il = illite, Or = orthoclase, Q = quartz, K = kaolinite.

After acid activation and pillaring treatment, the diffractogram clay treated samples have the same appearance to that of the raw clay. Several authors have shown that dilute acid treatment only partially destroys the basic structure of clay (Machéet *al.*, 2013; Nguetnkamet *al.*, 2005;

Christidiset *al.*, 1997). The peak at  $d = 10.27\text{Å}$  on the pillared clay diffractogram shows the presence of a more crystalline material, which is an indication of the presence of Al bridge between the Al- pillared montmorillonite sheets.

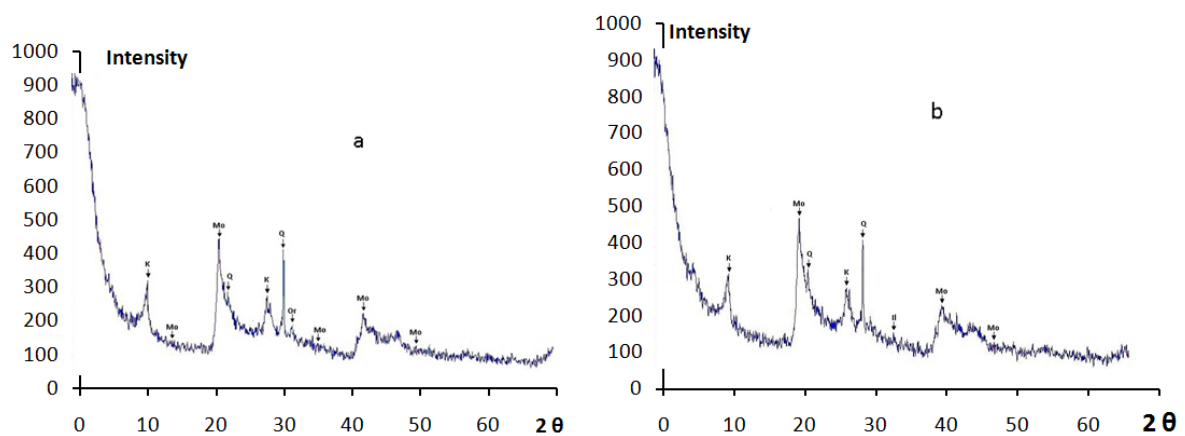


**Figure 2:** Diffractograms of activated (a) and pillared clays (b)

### Fourier transform infrared spectroscopy (FTIR) of clays

The IR spectra of 2  $\mu\text{m}$  and 50  $\mu\text{m}$  clay samples, as well as those of activated and pillared clays have the same appearance and show several bands characteristic of type 2:1 clays, particularly the band located in the range 3300 – 3750  $\text{cm}^{-1}$ , with shoulders between 3200 and 3500  $\text{cm}^{-1}$  and more intense around 3456  $\text{cm}^{-1}$  characteristic of the hydrophilic materials and corresponds to the vibrations of the OH groups of the water absorbed between the clay sheets; the double bands 3626 – 3670  $\text{cm}^{-1}$  and 3456 – 3626  $\text{cm}^{-1}$  O-H stretching of structural Al-OH, suggest the presence of type 2:1 clay. These results are in good agreement with the results of Chipera and Bish (2001) and Madejova and Komadel (2001). Furthermore, the band that spreads between 1600 – 1700  $\text{cm}^{-1}$  with the peak at 1638  $\text{cm}^{-1}$

is attributed to the valence vibrations of the OH group of the water absorbed between the montmorillonite layers. In addition, the intense band located between 900 – 1200  $\text{cm}^{-1}$  and centered at 1038  $\text{cm}^{-1}$  corresponds to the valence vibrations of the Si-O bond and is characteristic of aluminosilicates.

The acid and pillaring treatments of the clays reveal the Al-OH deformation vibrations around 801 and 915  $\text{cm}^{-1}$  and the Mg-O and Mg-OH vibrations merge with that of Si-O located at 698  $\text{cm}^{-1}$  (Bouraset *et al.*, 2007, Hidalgo *et al.*, 1995). These vibrations are characteristic of type 2:1 clay. In addition, the bands located at 541, 471 and 436  $\text{cm}^{-1}$  are attributed to the vibrations of the Si-O-Al, Si-O-Mg, and Si-O-Fe bonds, respectively and are indicative of the presence of exchangeable cations as presented in the chemical analysis.

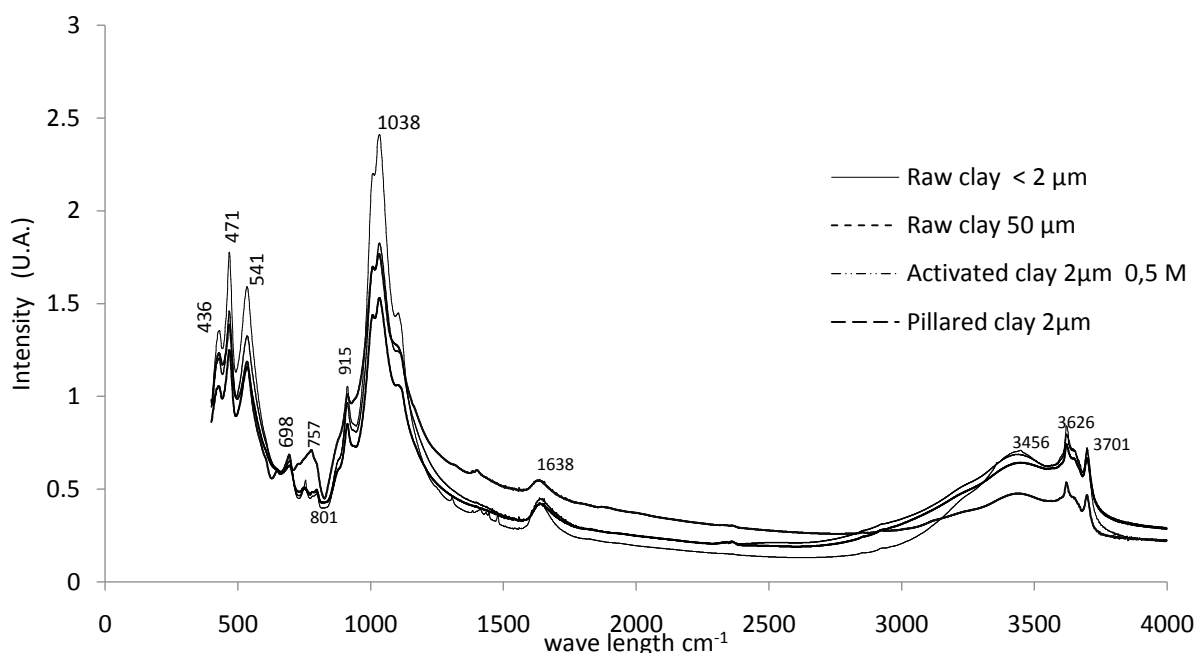
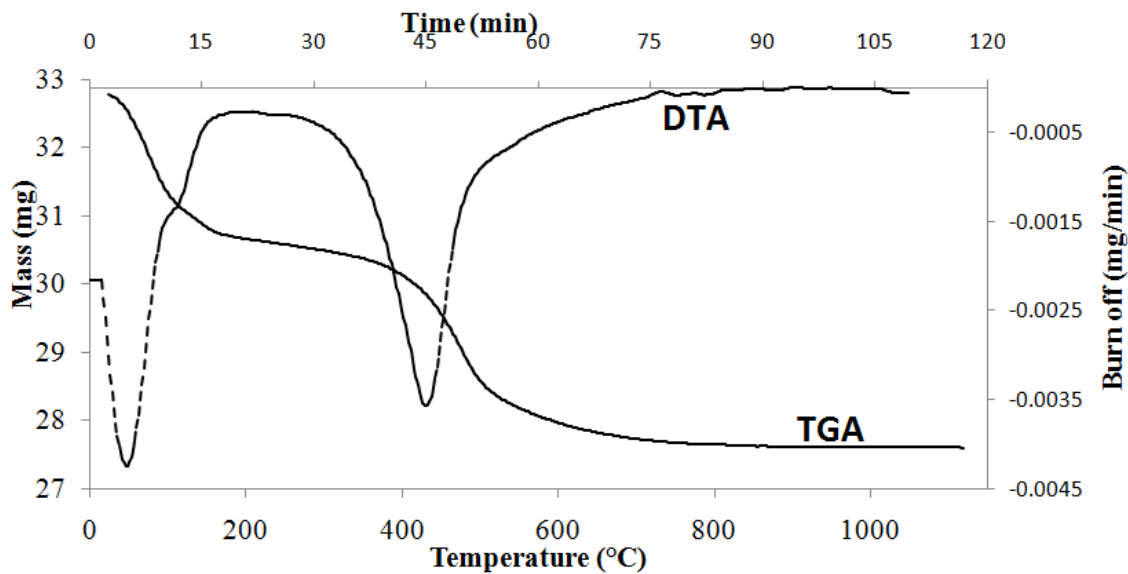


Figure 3: Infrared spectra of raw and modified clays

### Thermal Analysis (TGA, DTA)

Thermal analysis curves (DTA, TGA) of the raw clay (Figure 4) show two main endothermic peaks of mass loss. The first, between 50 and 120°C (5.3% of total mass loss) corresponds to elimination of adsorbed water from the clay surface, the second, between 120 and 260°C (1.4% of total mass loss) corresponds to the elimination of water between the clay layers. There is also a third peak between 260 and 700°C with a maximum at 480°C, which corresponds to the dehydroxylation of the clay.

Moreover, thermal analysis curves of modified clays show the disappearance of the endothermic peak at 150°C corresponding to the removal of water adsorbed on the surface of the clay. Kuila and Prasad (2013), observed that this peak, around 160°C in their study, corresponds to the removal of strong- electrostatically bound water associated with montmorillonite clays. In fact, the activation makes the clay more hydrophobic and promotes the elimination of water from the surface of the activated clay. In the case of pillared clay, aluminum polymers form bridges and reduce the interlayer space.



**Figure 4:** Thermal analysis of TGA and DTA analysis of raw clay

The TGA curves of the modified clays thus have only 2 mass losses (Table 2). These mass losses are about the same value for activated and pillared clays, but greater than the loss of mass of the raw clay. The high proportion of water is

attributed to the condensation of water in the pores of the activated clay and the presence of water in the polymers for aluminum pillared clay. Mass losses between 260°C and 700°C are greater for pillared clay than the other two clays.

**Table 2:** Thermal analysis (TGA and DTA) of raw and modified clays

Designation	Amount (mg)	Total mass loss (%)	Temperature (°C)	Partial mass loss (%)	T <sub>max</sub> (°C)
Raw Clay (ANB)	5.05	15.50	50 - 120	5.30	75
			120 - 260	1.40	110
			260 - 700	8.80	474
Activated clay 0,5M (A05)	5.63	16.70	50 - 240	8.09	73
			240 - 736	8.59	474
Pillared clay (APA)	5.89	17.35	50 - 240	8.31	73
			241 - 736	9.04	473

### SEM Analysis

The SEM images of the clay samples show a sheet-like structure. The raw clay sample (ANB) has a disordered morphology without any particular shape and elementary layers cannot be distinguished. Adjia (2012) also found that the morphology of alluvial clays in the far north of Cameroon is made of very fine clusters of irregularly sized and micron sized platelets.

In addition, the morphology of the clays is modified by the different treatments that clays undergo. Indeed, the layers are clearly visible on the A05 acid activated clay sample (Figure 5) which shows that acid treatment of clay has changed its morphology. The morphology of the pillared clay sample (APA) has a more compact sheet-like structure. This reflects a good insertion of polycations.

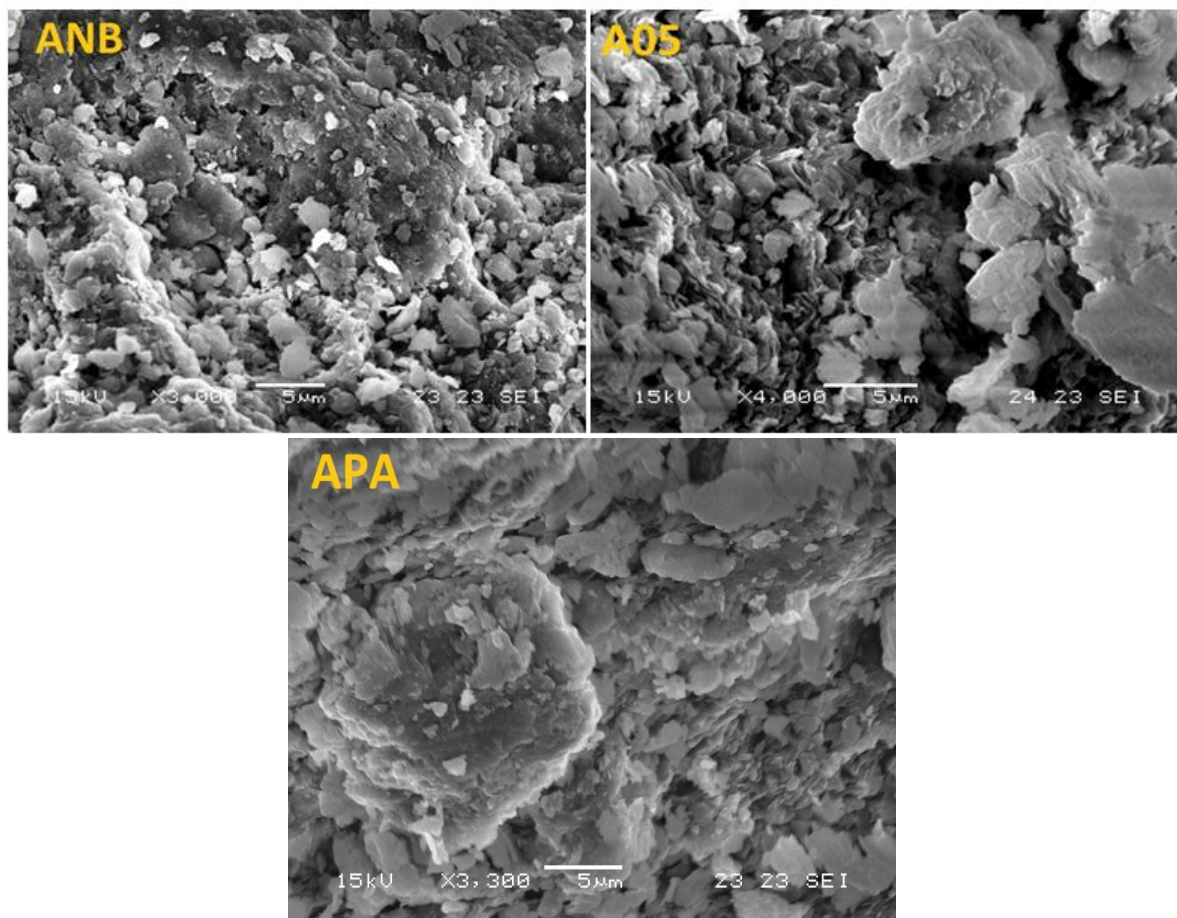
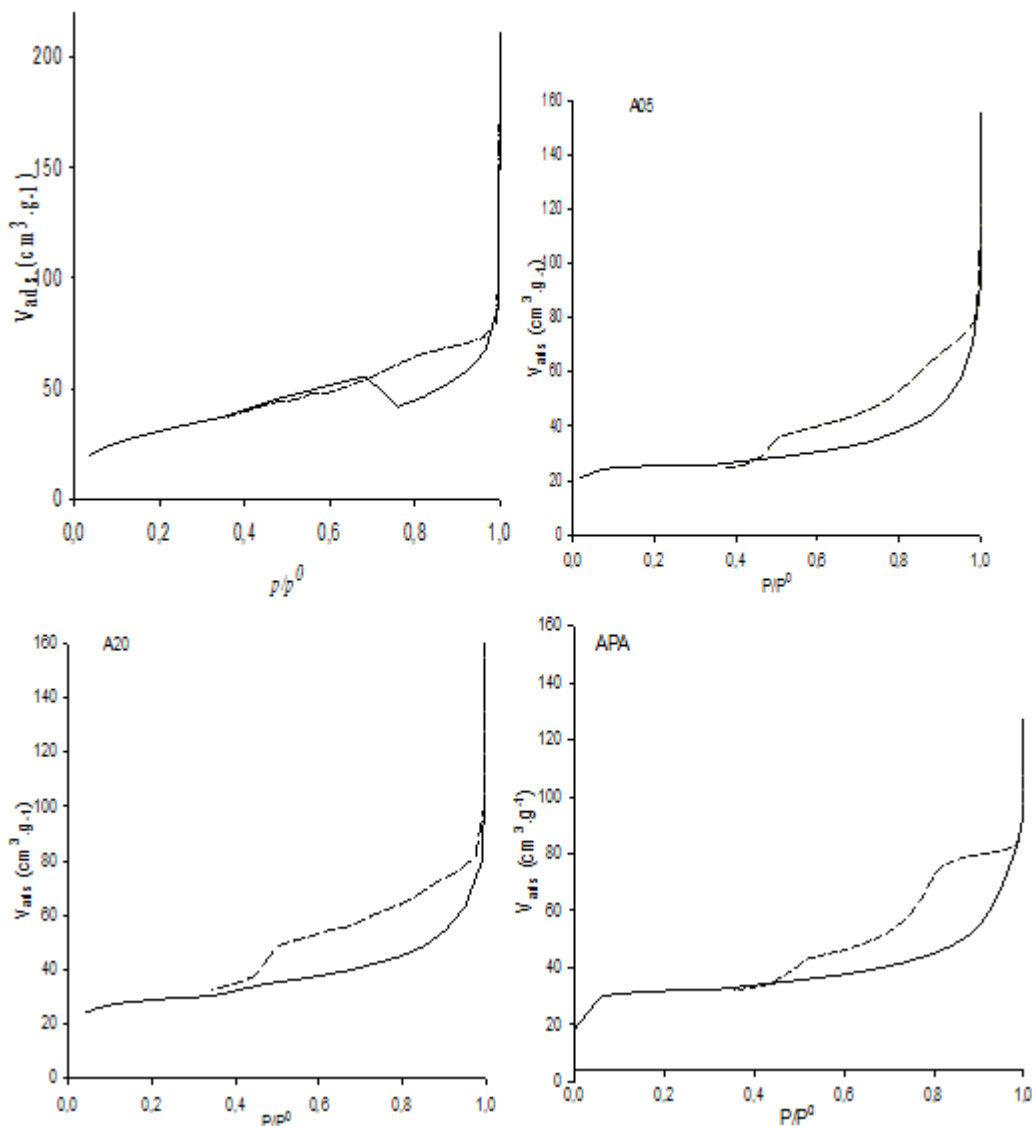


Figure 5: SEM micrographs of raw (ANB), acid activated (A05) and pillared (APA) clays

#### TEXTURAL PROPERTIES OF CLAYS

The isothermal curves of raw and modified clays are similar to those of type IV isotherms with hysteresis formation. The hysteresis is located between the  $P/P^{\circ}$  values of 0.70 and 0.95, which indicates that the pores are of size close to the mesopore domain. The acid and pillaring treatments favor a change in hysteresis towards the micropore region ( $P/P^{\circ} = 0.4$ ). The adsorption and desorption

isotherms form an asymptotic plane at the saturation pressure plane of the nitrogen  $P/P^{\circ}$ , which indicates a capillary condensation highlighting the presence of parallel cylindrical pores and macropores in the structure of the clay. These results are similar to those of Kuila and Prasa (2013) and Neamanet *al.*, (2003), who worked on a montmorillonite that show a presence of significant volumes of micropores, mesopores, and macropores.



**Figure 6:** Adsorption/desorption isotherms for raw (ANB), acid activated (A05&A20) and pillared (APA)clays

Adsorption/desorption isotherms allowed determination of internal parameters of clay samples, Table 3. The analysis of these values show that the BET surface area and pore volume of the raw clay (ANB) are of the same order of magnitude as the values generally found for montmorillonite (Perronet *et al.*, 2007; Nguetnkamet *et al.*, 2005). The surface area of the raw clay, however, is greater than that of 0.5 M H<sub>2</sub>SO<sub>4</sub>activated clay with. This reduction is not common, in fact, an increase in specific surface area is very often observed with the mineral acid treatment (Nguemtchouin, 2012). It can

be considered, however, that the reaction with H<sub>2</sub>SO<sub>4</sub> caused leaching of the amorphous material (feldspar, hydroxide, and carbonate), which contributed to the decrease in the specific surface of the raw clay. Moreover, the specific surface area of A20 clay is greater than that of A05 clay, which can be attributed to the formation of amorphous silica with the increase in the concentration of the mineral acid (Nguetnkamet *et al.*, 2005). The specific surface of pillared clay is greater than that of both acid activated clays. This can be attributed to the formation of Al bridges between the clay layers.

**Table 3: BET and BJH clays parameters**

Measured parameters	Adsorbents			
	ANB	A05	A20	APA
BET Surface (m <sup>2</sup> /g)	112	77	92	99
Pore volume (cm <sup>3</sup> /g)	0.088	0.077	0.083	0.097
Cumulated pore area (BJH) (m <sup>2</sup> /g)	80.7	64.5	78.5	65.9
Average pores diameter (BJH) (nm)	5.1	7.8	5.0	8.1

Table 4 shows average values of the pore size distribution. There is a disparity in the pore size distribution as a function of the treatments undergone by the clays.

**Table 4: Pore size distribution**

Pore size (nm)	Pore volume (cm <sup>3</sup> ·g <sup>-1</sup> ) / Percentage (%)							
	ANB		A05		A20		APA	
≤ 6	0.063	58.41	0.044	41.65	0.058	53.94	0.036	27.77
6 – 9	0.023	21.66	0.014	14.14	0.016	14.34	0.028	17.06
9 – 20	0.018	16.88	0.036	33.68	0.023	21.39	0.041	48.28
≥ 20	0.003	2.77	0.012	10.92	0.008	8.15	0.003	7.51
Total (cm <sup>3</sup> ·g <sup>-1</sup> )	0.105		0.104		0.105		0.108	

In fact, different treatments applied to the clays showed changes in the pore size distribution. The main consequence of activation was the decrease in percentage of pores of small size particles ( $\varnothing < 6$  nm). This decrease can be attributed to the leaching of exchangeable cations. The percentage of pore size between 6 and 9 nm for A05 represents 2/3 of these pores in ANB. On the other hand, the distribution of pores between 9 and 20 nm in A05 is twice than that of ANB. However, it can be considered that raw clay has no macropores because it contains only 2.8% of pores larger than 20 nm. In addition, pore size distribution of aluminium pillared clay is completely different from that of the other samples. Indeed, while pores smaller than 6 nm are more abundant in the other samples, pores with a size of between 9 and 20 nm are the most abundant in the pillared clay.

#### IV. CONCLUSION

The characterization of Far north Cameroon clay showed that is of swelling type. The results of the FTIR as well as the textural analysis confirmed that the clays are in the smectites family, with X-ray diffraction highlighting the presence of montmorillonite as main component. This type of clay is among the most widely used adsorbents in

water treatment (Rajani, 2011). Acid activation and pillaring lead to changes in the clays structural, textural, and surface energy properties. Indeed, the acid treatment partially destroys the structure of the clay and pillaring creates aluminum bridges between the layers of montmorillonite. These treatments induce the formation of an amorphous phase by the acid treatment and the presence of aluminum polymer for the pillared clay. In addition, the distribution of the mean pore size varies from 49 Å to 80 Å, which leads to the conclusion that clays consist mainly of mesopores. Pillaring treatment (APA) promotes the increase of pore volume (0.0205 cm<sup>3</sup>/g). The pore diameter of ≤ 6 nm decreases with different treatments, from 58.41% in raw clays (ANB) to 27.77% for the pillared clays (APA) in the benefit of the pores of sizes between 9 - 20 nm which increases from 16.88% in raw clays (ANB) to 48.28% for the pillared clays (APA). The specific surfaces although high in the raw clays (112 m<sup>2</sup>/g) due to the presence of amorphous material (feldspar, hydroxide, and carbonate) are decreasing after the acid treatment to 77 m<sup>2</sup>/g and after pillaring to 99 m<sup>2</sup>/g. This indicates that pillared clays, as presented by its characteristics, is the best matrix to use as an adsorbent in water treatment.

## DECLARATIONS

**Finance:** The work published here was funded by us and since we are in a very poor university it was not easy.

**Conflict of interest statement:** On behalf of all authors, the corresponding author states that there is no conflict of interest.

**Data availability statement:** data available in manuscript

## REFERENCES

- [1]. **Adjia Z.H., 2012.** Epuration des métaux lourds des eaux usées par les argiles alluviales de l'extrême-nord Cameroun. Thèse de doctorat en cotutelle, Université de Lorraine (France) - Université de Ngaoundéré (Cameroun), 290 p.
- [2]. **Adjia Z.H., Villiéras F., Kamga R., Thomas F., 2013.** Mineralogy and physicochemical properties of alluvial clays from far-north region of Cameroon: A tool for an environmental problem. *Int. J. Wat. Res. Env. Eng.*, vol 5 (1), 54-66.
- [3]. **Ahmaruzzaman, 2010; Ahmaruzzaman, M., 2010.** A review on the utilization of fly ash. *Prog. Energy Combust. Sci.* 36, 327-363
- [4]. **Alsbaiee, A., Smith, B.J., Xiao, L.L., Ling, Y.H., Helbling, D.E., Dichtel, W.R., 2016.** Rapid removal of organic micropollutants from water by a porous beta-cyclodextrin polymer. *Nature* 529, 190 – 146
- [5]. **AnuradhaAwasthi, PradipJadhao, KanchanKumari, (2019).** Clay nano-adsorbent: structures, applications and mechanism for water treatment. *SN Applied Sciences*, 1:1076, 21p
- [6]. **Babel S. and Kurniawan T.A., (2003),** Low-cost adsorbents for heavy metals uptake from contaminated water: a review. *J. of Hazard Mater*, 97,219–243
- [7]. **Basu, A., Mustafiz, S., Islam, M.R., Bjorndalen, N., Rahaman, M.S., Chaalal, O. (2006),** A Comprehensive Approach for Modeling Sorption of Lead and Cobalt Ions through Fish Scales as an Adsorbent. *Chemical Engineering Communications*,193, 580–605
- [8]. **Boldizar N., Măicăneanu A., Indolean C., Mânzatu C., Silaghi-Dumitrescu L., Majdik C., 2014.** Comparative study of Cd(II) biosorption on cultivated *Agaricusbisporus* and wild *Lactariuspiperatus* based biocomposites. Linear and nonlinear equilibrium modelling and kinetics. *Journal of the Taiwan Institute of Chemical Engineers* 45 (2014) 921–929
- [9]. **Bouras O., 2003.** Propriétés adsorbantes d'argiles pontées organophiles: synthèse et caractérisation. Thèse de doctorat, Université de Limoges, France, 162 p.
- [10]. **Bouras O., Bollinger J.C., Baudu M., Khalaf H., 2007.** Adsorption of diuron and its degradation products from aqueous solution by surfactant-modified pillared clays. *Appl. Clay Sci.*, 37 : 240-250
- [11]. **Chatain V., 2004.** Caractérisation de la mobilisation potentielle de l'arsenic et d'autres constituants inorganiques présents dans les sols issus d'un site minier aurifère. Thèse de doctorat de l'école doctorale de Chimie de Lyon - France, 189 p.
- [12]. **Chipera, S.J. and Bish, D.L. (2001)** Baseline studies of the clay minerals society source Clays: powder X-ray diffraction analysis. *Clays and Clay Minerals*, 49, 398–409
- [13]. **Christidis G.E., Scott P.W, Dunham A.C., 1997.** Acid activation and bleaching capacity of bentonites from the island of Milos and Chios, Aegean, Greece. *Appl. Clay Sci.*, 12, 329–347.
- [14]. **Damjanovic, L., Rakic, V., Rac, V., Stosic, D., Auroux, A., 2010.** The investigation of phenol removal from aqueous solutions by zeolites as solid adsorbents. *J. Hazard Mater.* 184, 477 – 484
- [15]. **De Boer JH, Linsen BG, Osinga TJ (1996).** Studies on pore systems in catalysts – Part VI: The universal curve. *J. Catal.* 4:643-648.
- [16]. **Delgado, L.F., Charles, P., Glucina, K., Morlay, C., 2012.** The removal of endocrine disrupting compounds, pharmaceutically activated compounds and cyanobacterial toxins during drinking water preparation using activated carbon-A review. *Sci. Total Environ.* 435, 509 – 525 .
- [17]. **Dias, J.M., Alvim-Ferraz, M.C.M., Almeida, M.F., Rivera-Utrilla, J., Sanchez-Polo, M., 2007.** Waste materials for activated carbon preparation and its use in aqueous phase treatment: a review. *J. Environ. Manag.* 85, 833 – 846
- [18]. **Dimple L., 2014.** Adsorption of Heavy Metals: A Review. *International Journal of Environmental Research and Development.* ISSN 2249-3131 Volume 4, Number 1, pp. 41-48
- [19]. **Eggen, R.I.L., Hollender, J., Joss, A., Scheffarer, M., Stamm, C., 2014.** Reducing the discharge of micropollutants in the aquatic environment: the benefits of upgrading wastewater treatment plants. *Environ. Sci. Technol.* 48, 7683 – 7689

- [20]. **Gerecke, A.C., Scharer, M., Singer, H.P., Müller, S.R., Schwarzenbach, R.P., Sägesser, M., Ochsenbein, U., Popow, G., 2002.** Sources of pesticides in surface waters in Switzerland: pesticide load through waste water treatment plantsecurrent situation and reduction potential. *Chemosphere* 48, 307 – 315
- [21]. **Hidalgo C., Thiry M., Elsass F., Quantin P., 1995.** Caractérisation minéralogique des argiles des sols volcaniques indurés (Tepetates) de la vallée de Mexico. *Scientifics registration*, 22 (2), 48-91.
- [22]. **Ibisi N. E. and Asoluka C. A. (2018).** Use of agro-waste (Musa paradisiaca peels) as a sustainable biosorbent for toxic metal ions removal from contaminated water. *Chemistry International* 4(1), 52-59
- [23]. **Kuila U. and Prasad M., 2013.** Specific surface area and pore-size distribution in clays and shales. *Geophysical Prospecting*, 61, 341–362
- [24]. **Kwon J.S., Yun S.T., Lee J.H., Kim S.O., Jo H.Y., 2010.** Removal of divalent heavy metals (Cd, Cu, Pb, and Zn) and arsenic (III) from aqueous solutions using scoria: kinetics and equilibrium of sorption. *J. of Hazard Mater*, 174, 307–313
- [25]. **Lefebvre, O., Moletta, R., 2006.** Treatment of organic pollution in industrial saline wastewater: a literature review. *Water Res.* 40, 3671 – 3682
- [26]. **Li M., Xiao X., Wang S., Zhang X., Li J., Spyros G. Pavlostathis, Luo X., Luo S., Zeng G. (2020).** Synergistic removal of cadmium and organic matter by a microalgaeendophyte symbiotic system (MESS): An approach to improve the application potential of plant-derived biosorbents. *Environmental Pollution*, 261, 114 – 177
- [27]. **Mache j. R., Signing P., Njoya A., Kunyukubundo F., Mbey J. A., Njopwouo D. and Fagel N. (2013).**Smectite clay from the Sabga deposit (Cameroon): mineralogical and physicochemical properties. *Clay Minerals*, 48, 499–512
- [28]. **Madejova J. and Komadel P. (2001).** Baseline studies of the clay minerals society source clays: infrared methods. *Clays and Clay Minerals*, Vol. 49, No. 5, 410–432
- [29]. **MenyaE., OlupotP.W., Storz H., Lubwama M., KirosY. (2018).** Production and performance of activated carbon from rice husks for removal of natural organic matter from water: A review. *Chemical Engineering Research and Design*, 129, 271-296
- [30]. **Michael, I., Rizzo, L., McArdell, C., Manaia, C., Merlin, C., Schwartz, T., Dagot, C., FattaKassinis, D., 2013.** Urban wastewater treatment plants as hotspots for the release of antibiotics in the environment: a review. *Water Res.* 47, 957 – 995
- [31]. **Mohan, D., Sarswat, A., Ok, Y. S., & Pittman, C. U. (2014).** Organic and inorganic contaminants removal from water with biochar, a renewable, low cost and sustainable adsorbent – A critical review. *Bioresource Technology*, 160, 191–202.
- [32]. **Mouthe A.G.A., Măicăneanu A., Bike Mbah J.B., Ndjeumi C.C., Cotet L.C., Kamga R., 2016.**Physico-chemical properties and crystal violet adsorption performances of h3po4 - modified mango seeds kernel. *Studia UBB Chemia*, LXI, 3, Tom I, 2016 (p. 195-214)
- [33]. **Nan Jiang, Ran Shang, Sebastiaan G.J. Heijman, Luuk C. Rietveld (2018)** High-silica zeolites for adsorption of organic micro-pollutants in water treatment: A review. *Water Research*, vol 144, pp 145 – 161
- [34]. **Ndjeumi C.C., Măicăneanu A., Bike Mbah J.B., Mouthe A.G.A., Kamga R., 2015.** Assessment of Physico-Chemical Parameters for Humic Acids Adsorption on Alumina. *AIS-Chemistry Journal*, Vol. 1, 4, 133-138
- [35]. **Neaman A., Pelletier M. et Villieras F. (2003).**The effects of exchanged cation, compression, heating and hydration on textural properties of bulk bentonite and its corresponding purified montmorillonite. *Applied Clay Science*, 22, 153– 168
- [36]. **Nguemtchouin M.M.G., 2012.** Formulation d'insecticides en poudre par adsorption des huiles essentielles de *Xylopiiaaethiopica* et de *Ocimumgratissimum* sur des argiles camerounaises modifiées. Thèse de doctorat en cotutelle de l'école nationale supérieure de chimie de Montpellier et de l'université de Ngaoundere. 293 p.
- [37]. **Nguetnkam J.P., Kamga R., Villieras F., Ekodeck G.E., Razafitianamaharavo A., Yvon J., 2005.**Assessment of the surface areass of silica and clay in acid-leached clay materials using concept of adsorption on heterogeneous surface. *J. Colloid Int. Sci.*, 289, 104-115.
- [38]. **Njoya A., Ekodeck G.E., Nkoumbou C., Njopwouo D. &Tchoua M. F., 2001.**Matériaux argileux au Cameroun: gisements et exploitation. Pp. 13 – 30 in : Actes de la Première Conférence sur la Valorisation des Matériaux Argileux au

- Cameroun (C. Nkoumbou & D. Njopwouo, editors). Yaoundé, Cameroun.
- [39]. **Njoya A., Nkoumbou C., Grosbois C., Njopwouo D., Njoya D., Courtin N.A., Yvon J. & Martin F., 2006.** Genesis of Mayouom kaolin deposit (West Cameroon). *Applied Clay Science*, 32, 125 – 140
- [40]. **Perronnet M., Villieras F., Jullien M., Razafitianamaharavo A., Raynal J. and Bonnin D., 2007.** Towards a link between the energetic heterogeneities of the edge faces of smectites and their stability in the context of metallic corrosion. *Geochimica et Cosmochimica Acta* 71, 1463–1479.
- [41]. **Pétard J., 1993.** Les méthodes d'analyses. Tome 1 : Analyse des sols. Orstom, Nouméa. Notes techniques, Lab commun Anal. 5. 192 p.
- [42]. **Rajani S., 2011.** Advances in Application of Natural Clay and Its Composites in Removal of Biological, Organic, and Inorganic Contaminants from Drinking Water. *Advances in Materials Science and Engineering*, Volume 2011, Article ID 872531, 17 pages. doi:10.1155/2011/872531
- [43]. **Rakic, V., Damjanovic, L., Rac, V., Stosic, D., Dondur, V., Auroux, A., 2010.** The adsorption of nicotine from aqueous solutions on different zeolite structures. *Water Res.* 44, 2047 – 2057
- [44]. **Reddy C.R., Bhat Y.S., Nagendrappa G., Jai Prakash B.S., 2008.** Bronsted and Lewis acidity of modified montmorillonite clay catalysts determined by FT-IR spectroscopy. *Catalyst Today*, 141: 157–160.
- [45]. **Rossner et al., 2009; Rossner, A., Snyder, S.A., Knappe, D.R.U., 2009.** Removal of emerging contaminants of concern by alternative adsorbents. *Water Res.* 43, 3787 – 3796
- [46]. **Snyder, S.A., Adham, S., Redding, A.M., Cannon, F.S., DeCarolis, J., Oppenheimer, J., Wert, E.C., Yoon, Y., 2007.** Role of membranes and activated carbon in the removal of endocrine disruptors and pharmaceuticals. *Desalination* 202, 156 – 181
- [47]. **Soumaya B.N., Mahmoud T., Mahamed H.F., 2009.** Activation d'une argile smectite tunisienne à l'acide sulfurique: Rôle catalytique de l'acide adsorbée par l'argile. *Journal de la Société Chimique de Tunisie*, 11: 191-203.
- [48]. **Srivastava, V.C., Swamy, M.M., Mall, I.D., Prasad, B., Mishra, I.M., 2006.** Adsorptive removal of phenol by bagasse fly ash and activated carbon: Equilibrium, kinetics and thermodynamics. *Colloids and Surfaces A: Physicochemical and Engineering Aspects*, 272: 89-104
- [49]. **Stackelberg, P.E., Gibs, J., Furlong, E.T., Meyer, M.T., Zaugg, S.D., Lippincott, R.L., 2007.** Efficiency of conventional drinking-water-treatment processes in removal of pharmaceuticals and other organic compounds. *Sci. Total Environ.* 377, 255 – 272
- [50]. **Talidi A., 2006.** Etude de l'élimination du Chrome et du bleu de méthylène en milieu aqueux par adsorption sur la pyrophyllite traitée et non traitée. Thèse de Doctorat. Université Mohammed V-Agdal, Maroc, 141 p.
- [51]. **Unuabonah E.I., Kayode O., Adebowale, Dawodu F.A., 2008.** Equilibrium, kinetic and sorber design studies on the adsorption of Aniline blue dye by sodium tetraborate-modified Kaolinite clay adsorbent. *J. Hazard. Mat.*, 157, 397-409.
- [52]. **Villieras F., Michot L. J., Bardot F., Chamerois M., Eypert-Blaison C., François M., Gérard G., Cases J.M., 2002.** Surface heterogeneity of minerals. *Comptes Rendus Geoscience*, 597–609.
- [53]. **Wibulswas R., White D. A., Rautiu R., 1998.** Removal of humic substances from water by alumina – based pillared clays. *Environmental technology*, vol. 19, 627-623.
- [54]. **Yadanaparthi S.K.R., Graybill D. and Wandruszka R., 2009.** Adsorbents for the removal of arsenic, cadmium, and lead from contaminated waters. *J. of Hazard Mater.*, 171, 1-15